Helsinki University of Technology
Espoo Finland

Thermal analysis of a synchronous generator taking into account the rotating high-frequency magnetic field harmonics

Y. Fujinami, S. Noguchi, H. Yamashita V. Cingoski

Faculty of Engineering, Hiroshima University
1-4-1 Kagamiyama, Higashihiroshima,
739-8527 Japan
Telephone +81 824 24 7665
Fax +81 824 22 7195
Email: fuji@eml.hiroshima-u.ac.jp
noguchi@eml.hiroshima-u.ac.jp
yama@eml.hiroshima-u.ac.jp

Electric Power Company of Macedonia
str. "11 Oktomvri" 9,
91 000 Skopje, Republic of Macedonia
Telephone +389 91 / 149 093
Fax +389 91 / 111 160
Email: vlatko@esmak.com.mk

ABSTRACT

To increase the efficiency of the rotating machines, it is very important to consider thermal field distribution during design stage. It is well known that even a small temperature increase beyond the normal operating level deteriorates rapidly the properties of the insulation materials and decreases drastically the lifetime of the windings. Therefore, it is necessary to throughout investigate the temperature rise in the rotating machines during initial design stage.
In this paper, we discuss a method for temperature field analysis inside the generators taking into account the high-frequency magnetic harmonics. The method is based on the 2D thermal field analysis using the finite element method. We show that taking into account the high-frequency magnetic harmonics, the accuracy of the computed temperature distribution could be improved. The high-frequency magnetic harmonics are considered for the accurate calculation of the iron loss inside each finite element. In this paper, we applied this method to a three-phase synchronous generator and the comparison between the computed and the measured results is shown.

1 INTRODUCTION

It is well known that the calculation of the temperature distribution in electrical machines is a very difficult problem. As far as the heat sources are concerned, apart from the ordinary copper losses, two additional sources, both with the electromagnetic origin, are the eddy currents in copper and iron parts, as well as the hysteresis in iron parts. In addition, due to the rotation of the rotor, it is extremely difficult to decide how to consider heat conduction in the air gap region between the rotor and stator. For this reason, many authors, in numerous number of papers such as those referred in this paper, tried to simplify the problem in order to calculate approximately the temperature rise, at least in the important parts or points of the machine.
In those papers, many assumptions are made for these approximate calculations; e.g., some authors consider only the stator or the rotor [1] – [4]. However, this is not usual since in this case to simulate a specific region special assumptions are to be made on the boundary. In some approaches [2], [3], an equivalent thermal conductivity for slot copper and slot insulation together is introduced. The other papers consider either the copper losses [4] or the iron losses [5], but not both type of losses in the same time. Unfortunately, using either one of the computation methods proposed in the above-mentioned papers, only the power supply frequency is taken into account for calculation of the iron loss. Because the hysteresis losses are in direct proportion to the power supply frequency and to the square of magnetic flux density, while the eddy current losses are in proportion to square of the power supply frequency and the magnetic flux density, assumption that magnetic flux density changes along sine curve is strongly justified. Therefore, the high-frequency magnetic harmonics in the teeth of the rotor and stator are neglected. However, in fact, it is well known that the high-frequency magnetic harmonics are always generated inside the teeth of the machine. Therefore, to neglect them cannot lead to an accurate simulation of the temperature distribution. In this paper, we present a procedure to increase the accuracy of the calculation of the iron losses taking into account the high-frequency magnetic harmonics. These iron losses, as can be shown later in this paper, have significant influence on analysis of the temperature distribution inside a synchronous generator.

2 SIMULATION METHOD

The procedure introduced in this paper for taking into account the high-frequency magnetic harmonics can be simply divided into several consecutive steps. First, we simulate a coupled numerical analysis of the magnetic field and the electric circuit by means of the 2D finite element method. Consequently, the magnetic field distribution inside the machine and the currents flowing inside the rotor and stator windings are obtained simultaneously. Next, the copper losses inside the windings are calculated using the previously computed results for the currents. In the same time, the iron losses inside the magnetic materials are calculated by taking into account the high-frequency magnetic field harmonics. Finally, the temperature distribution inside the rotating machine is computed using the computed copper and iron losses as the temperature field sources.

3 THERMAL ANALYSIS

The generated heat inside a rotating machine is caused by the generated copper and iron losses. The generated heat conducts inside the core of the machine and its windings. Beside conduc-

tions, on the outer surface of the machine and in the rotor's air slots, the heat transfers to the external air due to machine's natural cooling as a result of the rotation, or by means of forced cooling by the existing external fan. Finally, in the air gap region, the heat conducts and radiates. As can be notice, the distribution of the thermal heat inside the rotating machines is very complex. Fortunately, the influence of the thermal radiation inside the air gap region is very small and can be neglected. Moreover, there are no axial heat fluxes in the air gap region, because its width is too small to compare with its length. Consequently, the reasons, which influence the value of the thermal conductivity coefficient, are mainly the air gap length and the speed of the rotor. In this paper, the assumed value of the thermal conductivity coefficient is 0.0784 (W/mK) [2]. Because, the width of the insulation region between the core and the machine windings consisting of air and the insulation material is too small, we treat that the thermal conductivity coefficient is constant and has the value of 0.111 (W/mK) in the rotor, 0.094 (W/mK) in the stator.

It is also supposed that the component of the heat dissipation at the boundary has only a radial direction, which means that we supposed that there are no thermal currents perpendicular to the generator's cross section. Since the analysis region is symmetrical, modeling one pole with the appropriate cyclic symmetry conditions is sufficient. In this paper, the heat transfer boundary conditions were applied on the radial boundary, and the periodical boundary conditions were applied on the radius boundary where the temperature of each point on the boundary was equal to a designated correspondence point.

4 LOSSES

In this paper, we consider the copper losses in the windings and the iron losses in the magnetic core as the main heat sources inside the generator. We calculate these losses from the obtained current values and the magnetic flux density for one time cycle by the simulation of the magnetic and electric circuit coupled analysis.

4.1 COPPER LOSSES

The copper losses W_c are computed according to the following equation:

$$W_c = R\left(\sqrt{\frac{1}{T}\int_0^T i^2 dt}\right)^2 \qquad (1)$$

where R is the resistance of the winding, T is the period, and i is the instantaneous value of the current.

4.2 IRON LOSSES

The n-th high-frequency harmonics magnetic density obtained by expanding the magnetic flux density B^e using Fourier progression can be described as an ellipse as shown in Fig. 1. Therefore, it is the sums of two sine waves of 90 degrees phase difference and with amplitude of maximum value of the magnetic flux density. In this paper, we propose a method, which utilize calculation of the iron loss using these magnetic flux densities. Thus, in order to calculate the iron loss more accuracy, we determine n-th high-frequency harmonics magnetic densities $B^e_{n\max}$ and $B^e_{n\min}$, and then calculate the iron losses for each magnetic flux density value. Therefore, taking into consideration high-frequency harmonic magnetic density, the iron losses are computed by:

$$W_i^e = \sum_{n=1}^{\infty}\left\{p\left[K_h(B)nf{B^e_{n\max}}^2 + K_h(B)nf{B^e_{n\min}}^2\right]S^eL\right\} + \sum_{n=1}^{\infty}\left\{p\left[K_e(B)n^2f^2{B^e_{n\max}}^2 + K_e(B)n^2f^2{B^e_{n\min}}^2\right]S^eL\right\}, \qquad (2)$$

where p is the mass density, f is the power supply frequency, S^e is the area of each element, L is the axial length of the machine, n is the number of high-frequency harmonic, $K_h(B)$ and $K_e(B)$ are the coefficients of the specific hysteresis and eddy current losses, respectively. The first term stands for the hysteresis losses and the last term stands for the eddy current losses.

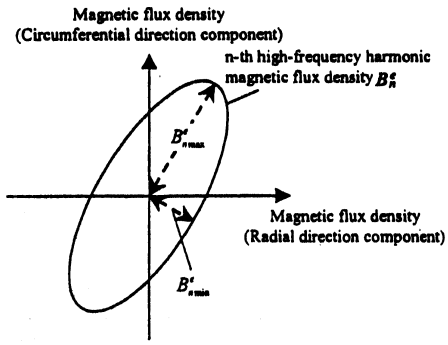

Fig. 1. N-th high-frequency harmonic of the magnetic flux density.

4.3 DETERMINING IRON LOSS COEFFICIENTS

Before calculating the iron losses using Eq. (2), the hysteresis loss coefficient $K_h(B)$ and the eddy current loss coefficient $K_e(B)$ in Eq. (2) must be determined. These coefficients can be determined from the measured *magnetic flux density – iron losses* curve at each frequency. First, it is known that the relation between the iron losses and the frequency are:

- Hysteresis losses are proportional to the frequency, and
- Eddy current losses are proportional to the square of the frequency.

Therefore, the relation between the hysteresis losses W_h and the eddy current losses W_e to the magnetic field frequency f' at magnetic flux density B can be described as in Fig. 2

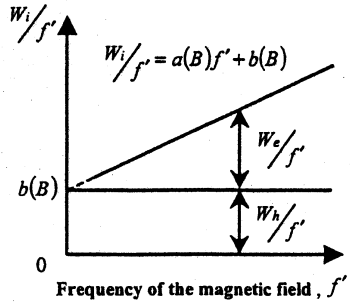

Fig. 2. The relation between the hysteresis and the eddy current losses to the magnetic field frequency.

If one determines the values $a(B)$ and $b(B)$ in Fig. 2, then, the coefficients $K_h(B)$ and $K_e(B)$ can be calculated using the relations given in Fig. 2. Therefore, in this paper, we use the following procedure:

STEP 1: Make a graph similar as that in Fig. 2 using the iron curve at each frequency.

STEP 2: Determine the values for $a(B)$ and $b(B)$ in Eq. (3) by minimum involution.

$$\frac{W_i}{f'} = a(B)f' + b(B) \quad , \tag{3}$$

where $a(B)$ and $b(B)$ are the constant values which depend on the magnetic flux density B.

STEP 3: Express the hysteresis losses W_h and the eddy current losses W_e simply as following:

$$W_h = p\left[K_h(B)nfB^2\right]SL \quad , \tag{4}$$

$$W_e = p\left[K_e(B)n^2f^2B^2\right]SL \quad . \tag{5}$$

Moreover, from Fig. 2 it is clear the following relationships

$$b(B) = \frac{W_h}{f'} \quad , \tag{6}$$

$$a(B)f' = \frac{W_e}{f'} \quad . \tag{7}$$

STEP 4: Determine the hysteresis losses coefficient $K_h(B)$ and the eddy current losses coefficient $K_e(B)$ for the particular values of the magnetic flux density, using equations Eq. (4) through (7).

Using the above-described procedure for several magnetic flux densities, we can determine the hysteresis losses coefficient $K_h(B)$ and the eddy current losses coefficient $K_e(B)$. Figure 3 shows typical graphical representation of the computed values of the coefficients $K_h(B)$ and $K_e(B)$.

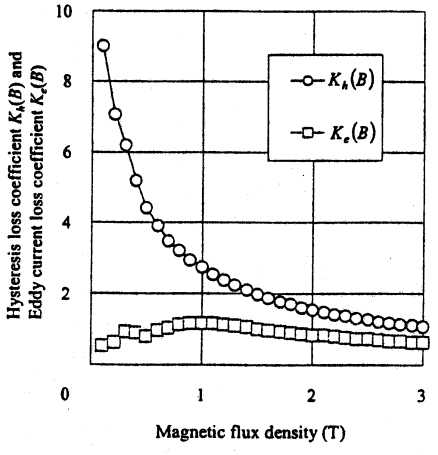

Fig. 3. Hysteresis loss coefficient $K_h(B)$ and eddy current loss coefficient $K_e(B)$.

5 RESULTS

As a computation model, we used a four pole self-excited synchronous generator shown in Fig. 4. We analyzed 25 [kVA], 220 [V] generator in the steady-state operation mode with rated load at $\cos\phi$ =0.8.

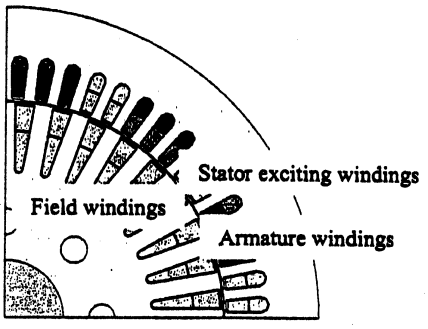

Fig. 4. Calculation model.

5.1 LOSS CALCULATION

First, we computed the generated heat as the post-processing routine after the magnetic field-electric circuit coupled analysis is performed. The comparison between the experimental (measured) results and the computed results for copper losses and iron losses are given in Table 1 and Table 2, respectively. Moreover, the obtained iron losses distribution is shown in Fig. 5.

Table 1. Comparison between measured and computed values for copper losses.

	Armature	Stator exciting	Field	Total
Computation (W)	1055	472	1566	3093
Experiment (W)	915	448	1301	2664

Table 2. Comparison between measured and computed values for iron losses.

	Hysteresis	Eddy current	Total
Computation (W)	413	430	843
Experiment (W)	---	---	806

Table 1 and Table 2 show that the results of computation are higher than that of the experiment, because we didn't consider a skew effect. If we consider the skew effect, the high-frequency harmonic components of the armature voltage will disappear. Therefore, the copper and the iron losses will be reduced because of the reduction of the armature currents. Fig. 5 shows that the large amount of losses is generated inside the teeth of the rotor and stator. It is clear that the value of losses depends on the high-frequency magnetic harmonics. Therefore, we investigate the high-frequency magnetic harmonics as to the magnetic flux density using Fourier progression inside the teeth of the rotor (1), stator (2), and shaft (3) (see Fig. 6). The loci of the main high-frequency harmonic components of the magnetic flux density and the original magnetic flux density inside the teeth of the rotor, stator, and the machine shaft are described in Fig. 7, 8 and Fig, respectively. Fig. 7 shows that the locus of the

30-th elliptical magnetic flux density is clearly generated because the rotor teeth cross 30 slots of the stator during rotation of the rotor. This is equal as to take into consideration the high-frequency magnetic harmonics. Moreover, in case of Fig. 8, the locus of the first elliptical magnetic flux density is generated clearly because the armature voltage is higher than the stator exciting voltage. However, Fig. 8 also shows that the loci of the 17-th, 18-th, and 19-th elliptical magnetic flux density are also generated because the stator teeth cross the 18 slots of the rotor in the process of rotation of the machine. This is again equal as we consider the high-frequency magnetic harmonics. Fig. 9 shows that the change of the magnetic flux density is fewer than that inside of the rotor and stator teeth. It also shows that the locus of the 3-th elliptical magnetic flux density is generated. The armature windings don't have any influence on the rotor because the field windings and the armature windings are both four-pole windings. However, the stator windings, which are twelve-pole windings show some influence on the rotor windings that are four-pole windings.

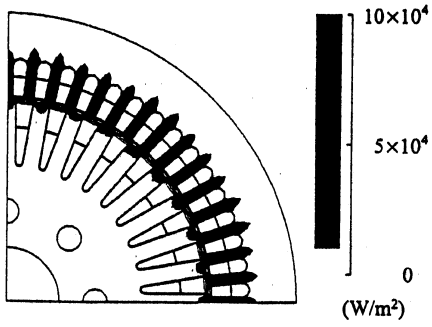

Fig. 5. Computed iron loss distribution.

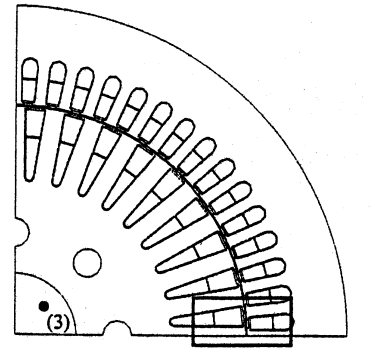

(a) Outline of the investigated region.

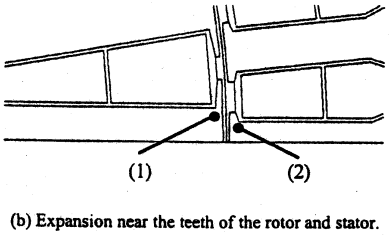

(b) Expansion near the teeth of the rotor and stator.

Fig. 6. Investigated elements for high-frequency harmonics analysis.

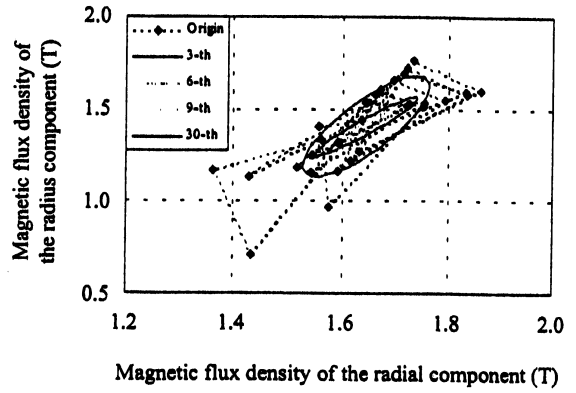

Fig. 7. Loci of the main high-frequency harmonic components of the magnetic flux density and the original magnetic flux density inside the teeth of the rotor (1).

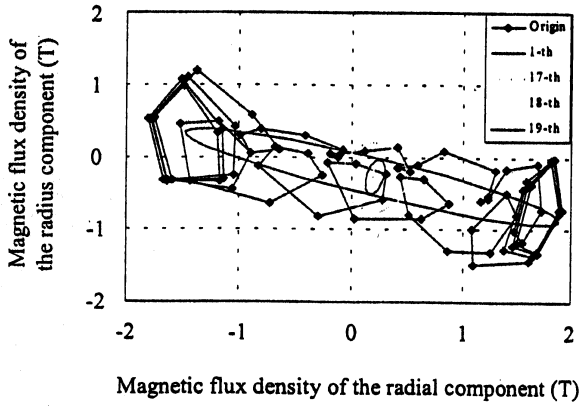

Fig. 8. Loci of the main high-frequency harmonic components of the magnetic flux density and the original magnetic flux density inside the teeth of the stator (2).

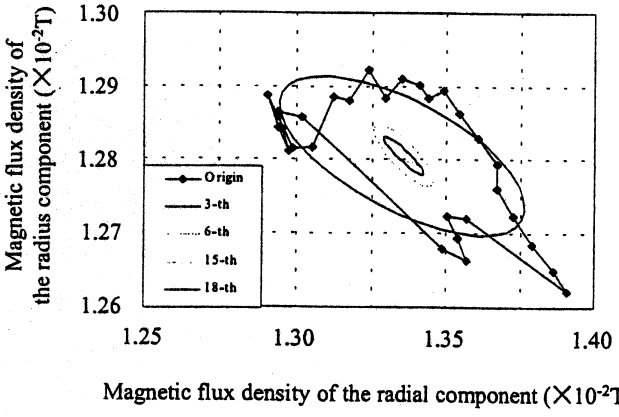

Fig. 9. Loci of the main high-frequency harmonic components of the magnetic flux density and the original magnetic flux density inside the shaft (3).

5.2 TEMPERATURE DISTRIBUTION

Next, we analyzed the temperature field distribution using finite element method utilizing the computed copper and iron losses obtained before. In heat conduction problem, the periodical boundary conditions were applied along lines *a* and *b*, while the heat transfer boundary conditions were applied along line *c* of the model (see Fig. 10). The thermal conductivities at each region are shown in Table 3. The convection heat transfer coefficient on the outer surface of the stator is 39.5 (W/m^2K), and 38.5 (W/m^2K) for the air slots inside the rotor. The computed temperature distribution is shown in Fig. 11. The comparison between the experimental and the computed results is given in Table 4. The temperatures inside the copper are the average values over the entire length of the windings. Table 4 shows that the computation results are higher than those obtained from the experiment, mainly because the calculated copper losses and iron loss are higher than the experimental.

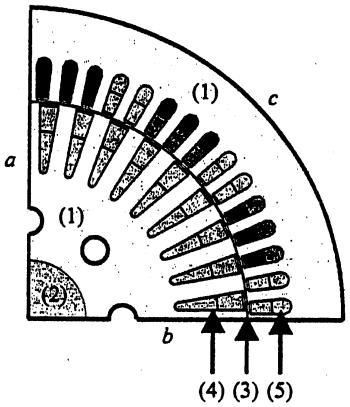

Fig. 10. Calculation model for temperature distribution.

Table 3. Thermal conductivity

No.	Region	Thermal conductivity(W/mK)
(1)	Iron	42
(2)	Shaft	53
(3)	Air gap	0.0784 [6]
(4)	Insulation of the rotor	0.111
(5)	Insulation of the stator	0.094

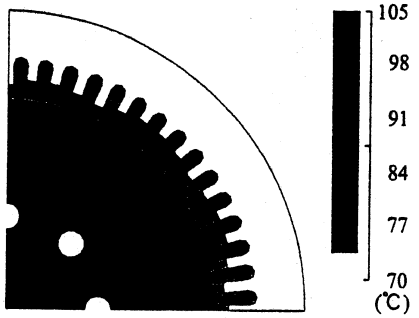

Fig. 11. Computed temperature distribution.

Table 4. Comparison between the temperatures obtained by computation and by experiments.

	Armature	Stator exciting	Field
Computation (℃)	77.5	75.9	89.3
Experiment (℃)	65.0	64.6	76.9

6 CONCLUSION

We described a method that takes into account the high-frequency magnetic harmonics for the thermal field computation. First, we calculated the distribution of the iron and copper losses. As a result, the high-frequency magnetic harmonics revealed. Therefore, we investigate the high-frequency magnetic harmonics of the magnetic flux density using Fourier progression inside the stator and rotor teeth and the shaft of the machine. Inside the teeth of the rotor, 30-th elliptical magnetic flux density was found, while for the stator, 17-th, 18-th and 19-th elliptical magnetic flux density was observed. This shows that the high-frequency magnetic harmonics should be considered. Finally, we computed the temperature distribution inside the synchronous generator taking into account previously obtained high-frequency magnetic harmonics. The results of the computation were compared with those obtained by the experiment and were higher than the measurements, mainly because the rotor skewing was neglected.

REFERENCES

[1] A. F. Armor, "Transient, three-dimensional, finite-element analysis of heat flow in turbine generator rotors", *IEEE Transactions on PAS*, Vol. PAS-99, No. 3, 1980, pp. 934-947.

[2] D. Sarker, P. K. Mukherjee, S. K. Sen, "Temperature rise of an Induction Motor during plugging", *IEEE Transaction on Energy Conversion*, Vol. 7, No. 1, 1992, pp. 116-124.

[3] D. Sarker, P. K. Mukherjee, S. K. Sen, "Approximate analysis of steady state heat conduction in an induction motor", *IEEE Transaction on Energy Conversion*, Vol. 8, No. 1, 1993, pp. 78-84.

[4] V. K. Garg, J. Raymond, "Magneto-thermal coupled analysis of canned induction motor", *IEEE Transactions on Energy Conversion*, Vol. EC-5, No. 1, (1986), pp. 110-114.

[5] Y. Lee, H. Lee and S. Hahn, "Temperature Analysis of Induction Motor with Distributed Heat Sources by Finite Element Method", *IEEE Transactions on Magnetics*, Vol. 33, No. 2, (1997), pp. 1718-1721.

[6] V. Hatziathanassiou, J. Xyteras and G. Archontoulakis, "Electrical-thermal coupled calculation of an asynchronous machine", *Archiv fur Electrotechnik* 77 (1994), pp. 117-122.